Strain-Induced Landau Levels in Arbitrary Dimensions with an Exact Spectrum

Stephan Rachel,[1] Ilja Göthel,[1] Daniel P. Arovas,[2] and Matthias Vojta[1]
[1]Institut für Theoretische Physik, Technische Universität Dresden, 01062 Dresden, Germany
[2]Department of Physics, University of California, San Diego, La Jolla, California 92093, USA
(Received 6 September 2016; published 21 December 2016)

Certain nonuniform strain applied to graphene flakes has been shown to induce pseudo-Landau levels in the single-particle spectrum, which can be rationalized in terms of a pseudomagnetic field for electrons near the Dirac points. However, this Landau level structure is, in general, approximate and restricted to low energies. Here, we introduce a family of strained bipartite tight-binding models in arbitrary spatial dimension d and analytically prove that their entire spectrum consists of perfectly degenerate pseudo-Landau levels. This construction generalizes the case of triaxial strain on graphene's honeycomb lattice to arbitrary d; in $d = 3$, our model corresponds to tetraxial strain on the diamond lattice. We discuss general aspects of pseudo-Landau levels in arbitrary d.

DOI: 10.1103/PhysRevLett.117.266801

Introduction.—The engineering of quantum phases and their properties has become an important concept in condensed matter physics. In this approach, one either builds or influences a large quantum system in a controlled fashion such that it displays properties not present in naturally occurring systems. Prominent examples are artificial lattices of atoms or molecules absorbed on surfaces [1], heterostructures made, e.g., from correlated-electron materials [2,3], and coupled-wire constructions of topological states of matter [4].

A particularly interesting tool, applicable to bulk materials, is lattice strain which—in a tight-binding description of electron dynamics—induces inhomogeneous hopping energies. In the context of graphene, it has been theoretically shown [5–7] that such inhomogeneous hopping mimics the effect of a vector potential in Dirac-fermion systems. If the resulting pseudomagnetic field is sufficiently homogeneous—applying, e.g., to triaxial strain patterns—it can induce single-particle pseudo-Landau levels (PLLs) very similar to Landau levels in a physical magnetic field. Such PLLs have indeed been observed in strained graphene flakes [8] as well as in artificial molecular structures [1]. However, the resulting spectral quantization is approximate and restricted to energies near the Dirac point. Nonuniform strain has also been discussed for Weyl semimetals, but controlled effects are again restricted to the low-energy part of the spectrum [9–11].

In this Letter, we lay out a scheme for strain engineering of single-particle levels which overcomes previous restrictions. We introduce tight-binding models with inhomogeneous hopping energies, defined on specific d-dimensional bipartite finite-size lattices, which display perfectly degenerate PLLs throughout their entire spectra. In $d = 2$, our model resembles triaxial strain applied to the honeycomb lattice in the limit of strong electron-lattice coupling [12], and we present the generalization to arbitrary d. Using iterative constructions, we are able to obtain the single-particle energies and their degeneracies in a closed algebraic form. Most remarkably, our scheme paves the way to Landau level physics in three dimensions, realizable via tetraxial strain applied to the diamond lattice.

Model.—Our tight-binding models are defined on a d-dimensional bipartite lattice, with sublattices A and B and coordination number $(d+1)$. The nearest-neighbor vectors $\hat{\boldsymbol{\delta}}_j$ connect the center of a $(d+1)$ simplex to each of its vertices and, in the absence of strain, satisfy $\hat{\boldsymbol{\delta}}_j^2 = 1$, $\hat{\boldsymbol{\delta}}_j \cdot \hat{\boldsymbol{\delta}}_{j'} = -(1/d)$ for $j \neq j'$, and $\sum_{j=1}^{d+1} \hat{\boldsymbol{\delta}}_j = \mathbf{0}$. In $d = 1, 2, 3$, the relevant simplices are line segment, triangle, and tetrahedron, respectively. The nearest-neighbor hopping Hamiltonian reads

$$H = \sum_{\boldsymbol{r}\in B} \sum_{j=1}^{d+1} t_{\boldsymbol{r},j}^{(N)} c_{\boldsymbol{r}}^{\dagger} c_{\boldsymbol{r}+\hat{\boldsymbol{\delta}}_j} + \text{H.c.}, \tag{1}$$

where $N = 1, 2, 3, \ldots$ specifies the linear system size. In the presence of strain, we continue to use the coordinates of the unstrained lattice. Key ingredients are the inhomogeneous hopping amplitudes

$$t_{\boldsymbol{r},j}^{(N)} = \frac{N - 1 - d\boldsymbol{r} \cdot \hat{\boldsymbol{\delta}}_j}{d+1}; \tag{2}$$

these can be generated by specific nonuniform strain in the limit of strong electron-lattice coupling [13]. In Eq. (2), $\boldsymbol{r} = 0$ defines the center of the system, and B sites are placed such that $t_{\boldsymbol{r},j}^{(N)}$ is integer. The scalar product leads to a linear spatial variation of hopping amplitudes. The hopping pattern (2) is such that a set of $t_{\boldsymbol{r},j}^{(N)}$'s vanish identically, naturally cutting out a piece of size N, with the overall shape of the d simplex, from a large lattice [12,13]; see Fig. 1.

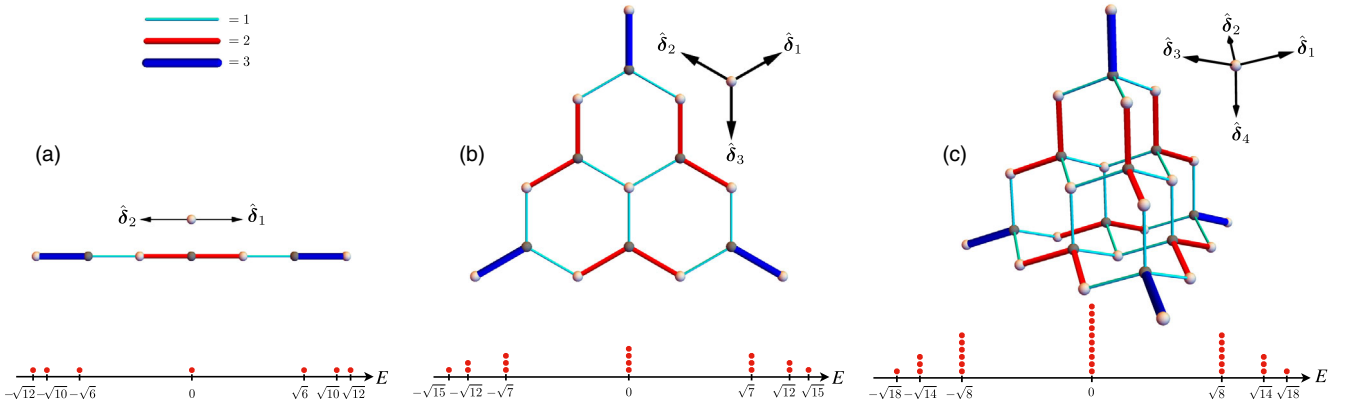

FIG. 1. Finite-size lattices (top) and their spectra (bottom) for $N = 4$ and (a) $d = 1$, (b) $d = 2$, and (c) $d = 3$. The hopping amplitudes $t^{(N)}_{\boldsymbol{r},j}$, Eq. (2), are indicated via line thickness and color (see the inset). The next outer bonds have a vanishing amplitude, thus cutting out (a) a line segment, (b) a triangle, and (c) a tetrahedron, each of linear size N. Note that unstrained lattices are shown; for finite electron-lattice coupling, weak (strong) bonds would be elongated (compressed). The energy levels and their degeneracies are given in Eqs. (3) and (4), respectively; for details, see the text.

As proven below, the level spectrum of H reads

$$E^{\pm}_n = \pm\sqrt{N(N+d-2) - n(n+d-2)} \qquad (3)$$

for $n = 1, \ldots, N-1$, and $E_N = 0$—this is the central result of this Letter. For $N \gg 1$ and $m = N - n \ll N$, the spectrum can be approximated by $\epsilon^{\pm}_m \equiv E^{\pm}_{N-m} \approx \pm\sqrt{2Nm}$. This corresponds to the low-energy spectrum of Dirac electrons subject to a vector potential; i.e., the $\sqrt{m}$ behavior can be interpreted in terms of Dirac Landau levels in d dimensions. The degeneracy of each energy $E^{\pm}_n$ is given by

$$z_{d,n} = \frac{n(n+1)(n+2)\ldots(n+d-2)}{(d-1)!}, \qquad (4)$$

which is $O(n^{d-1})$; specifically, $z_{1,n} = 1$, $z_{2,n} = n$, and $z_{3,n} = n(n+1)/2$. In Fig. 1, we display the corresponding lattices as well as the level spectra for $N = 4$.

We note that, to simplify expressions, Eq. (2) is scaled to yield integer $t^{(N)}_{\boldsymbol{r},j}$ and E^2_n; this results in a bandwidth $\propto N$. To obtain a spectrum with finite bandwidth for $N \to \infty$ requires us to rescale $t \to t/N$. Then, the low-energy levels follow $|\epsilon^{\pm}_m| \approx \sqrt{2m/N}$, corresponding to a pseudomagnetic field which scales as $1/N$.

We now discuss the three important cases $d = 1$, 2, 3 separately; in the remainder of this Letter, we prove the spectral properties for arbitrary d.

One-dimensional PLLs.—In $d = 1$, the discrete energy levels $E^{\pm}_n = \pm\sqrt{N(N-1) - n(n-1)}$ are nondegenerate, Eq. (4). Nevertheless, the term "Landau level" appears justified given that the low-energy spectrum emulates a one-dimensional Dirac theory coupled to a vector potential of a homogeneous magnetic field. The lattice, Fig. 1(a), is that of a two-atomic chain with an inhomogeneous Peierls-like distortion which increases away from the chain center. In analogy to $d = 2$, 3, one can interpret this hopping modulation as arising from biaxial strain; however, such a strain pattern cannot be realized using force fields in a solid. The $d = 1$ case is mainly interesting as a toy model.

Two-dimensional PLLs.—The $d = 2$ case corresponds to triaxial strain, Fig. 2(a), applied to graphene [1,6–8] in the limit of strong electron-lattice coupling [12,13]. This limit, together with the specific sample shape, yields perfectly degenerate levels in the *entire* spectrum following the exact expression (3), $E^{\pm}_n = \pm\sqrt{N^2 - n^2}$, Fig. 1(b). This is to be contrasted with PLLs for weak electron-lattice coupling which are smeared and restricted to low energies [1,6,8,14]. In the Supplemental Material [13], we illustrate the evolution between the two limits.

Three-dimensional PLLs.—The most interesting case is $d = 3$, which corresponds to *tetraxial* strain applied to a diamond lattice. First, we recall that a tight-binding model (of s orbitals, as opposed to the hybridized sp^3 orbitals of diamond) on the diamond lattice features a partial Dirac-type

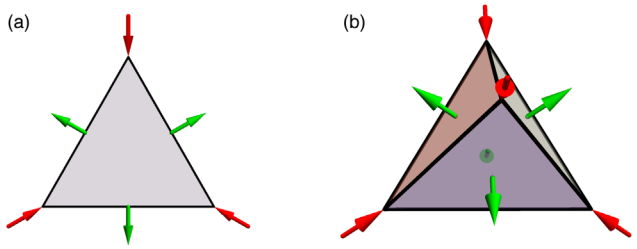

FIG. 2. Schematic illustration of forces for (a) triaxial strain applied to a triangle and (b) tetraxial strain applied to a tetrahedron. The resulting displacement fields are (a) $\boldsymbol{u}_{2D} = \bar{C}(2xy, x^2 - y^2)^T$ and (b) $\boldsymbol{u}_{3D} = \bar{C}(yz, zx, xy)^T$, where $\bar{C}$ is a constant.

band touching at the X points [15]. Second, the displacement vector for tetraxial strain, Fig. 2(b), is $\boldsymbol{u}_{3D} = \bar{C}(yz, zx, xy)$. In the limit of strong electron-lattice coupling, tetraxial strain leads to hopping modulations, as in Eq. (2). The resulting spectrum, $E_n^{\pm} = \pm\sqrt{N(N+1) - n(n+1)}$, is naturally interpreted as that of Landau levels in three spatial dimensions; see Fig. 1(c). The corresponding continuum theory and its consequences will be published elsewhere [16]. We have estimated that, for realistic electron-lattice coupling, 5% strain should be sufficient to produce visible Landau levels [13]. The construction of PLLs in $d = 3$ is interesting on fundamental grounds, given that the quantum Hall effect exists only for an even d; hence, Landau levels in $d = 3$ cannot be realized using physical magnetic fields.

Proof of the spectral properties.—In order to prove Eqs. (3) and (4), we start with general properties of bipartite graphs and their implications. Then, we use these properties in combination with Eq. (2) to iteratively construct the full spectrum. Further details of the proof are given in the Supplemental Material [13].

Bipartite hopping and eigenmodes.—Consider an arbitrary lattice, with all sites distributed into two sets, called the sublattices A and B. A hopping Hamiltonian whose only nonzero matrix elements connect the A and B sites defines a bipartite hopping problem. The corresponding real Hamiltonian matrix $\mathcal{H}$ in a site basis, with A sites arranged before B sites, consists of off-diagonal blocks. As a result, the spectrum is particle-hole symmetric; i.e., nonzero eigenvalues always come in pairs involving E and $(-E)$.

If there is an imbalance of the number of sublattice sites, i.e., $n_A \neq n_B$, there must be $|n_A - n_B|$ eigenvalues which vanish ($E = 0$), with eigenvectors localized on sublattice B if $n_B > n_A$ [17]. The existence of zero modes was first noted by Sutherland [18] and Lieb [19]; a simple proof is given in Ref. [20].

A further consequence of the bipartiteness is that the matrix $\mathcal{H}^2$ decouples into two disconnected blocks for the A and B sublattices. The eigenvalues of $\mathcal{H}^2$ are non-negative; the positive ones must be twofold degenerate [17], with one eigenvector solely defined on sublattice A and the other one on sublattice B.

Notation.—We denote the Hamiltonian matrix of Eq. (1) for linear size N as $\mathcal{H}_N$. To establish the spectrum (3), we prove that $\mathcal{H}_N^2$ possesses eigenvalues $(E_n^{\pm})^2 \equiv E_n^2$ that are $2z_{d,n}$-fold and $E_N^2 = 0$ $z_{d,N}$-fold degenerate. We denote the eigenvectors of $\mathcal{H}_N$ as $\psi_N^{(n,\mu)}$ and that of $\mathcal{H}_N^2$ as $\phi_N^{(n,\nu)}$, where μ, ν label degenerate eigenvectors. As noted, the positive-energy eigenvectors of $\mathcal{H}_N^2$ come in pairs, $\phi_{N,A}^{(n,\mu)}$ and $\phi_{N,B}^{(n,\mu)}$, which have vanishing amplitudes on sublattices B and A, respectively. Bipartite hopping implies that $\mathcal{H}_N$ maps the two eigenstates onto each other [21]:

$$\mathcal{H}_N \phi_{N,A}^{(n,\mu)} = E_n \phi_{N,B}^{(n,\mu)} \quad \text{and} \quad \mathcal{H}_N \phi_{N,B}^{(n,\mu)} = E_n \phi_{N,A}^{(n,\mu)}. \tag{5}$$

Note that Eq. (5) is true for arbitrary bipartite hopping problems: It is a consequence of $\mathcal{H}_N$ connecting only the A and B sites and the eigenvalue condition $\mathcal{H}_N^2 \phi_N^{(n)} = E_n^2 \phi_N^{(n)}$.

For future reference, we label the two nonzero blocks of the matrix $\mathcal{H}_N^2$ as A_N and B_N, $\mathcal{H}_N^2 = A_N \oplus B_N$, corresponding to its action on the A and B sublattices, respectively. Also, the sublattice with excess sites will be denoted B; the full expressions for the number of lattice sites for given N's and d's are provided in the Supplemental Material [13].

Iterative construction of the spectrum.—Step 1: For $N = 1$, the lattice consists of a single B site, and we have $\mathcal{H}_1 = \mathcal{H}_1^2 = B_1 = 0$, $E_1 = 0$, and $\phi_1^{(N=1)} = \psi_1^{(N=1)} = 1$. (It will become clear below that $\phi_N^{(N)} = \psi_N^{(N)}$ for an arbitrary N.)

Step 2: We now show that the matrix B_{N-1} is *identical* to A_N up to a constant shift,

$$A_N = B_{N-1} + \lambda(N) \cdot \mathbb{1}, \tag{6}$$

where $\lambda(N) = 2N + d - 3$ and $\mathbb{1}$ is the corresponding unit matrix; the matrix dimensions of A_N and B_N are given in the Supplemental Material [13]. As a result of Eq. (6), the eigenvectors of B_{N-1} and A_N are identical.

To prove Eq. (6), we first note that the positions of the B sites for system size N correspond to that of the A sites for the size $(N+1)$. Second, B sites have neighboring sites in the $(d+1)$ $\hat{\boldsymbol{\delta}}_j$ directions, while A sites have neighbors in the $(-\hat{\boldsymbol{\delta}}_j)$ directions. Therefore, the network of bonds between the A and B sites has been locally inverted when switching from system size N to $(N+1)$; see Fig. 3.

Consider now a B site for size N which is connected to its neighbors along the $(d+1)$ $\hat{\boldsymbol{\delta}}_j$ directions via the bonds of amplitudes $t_{\boldsymbol{r},j}^{(N)} \in \mathbb{N}$. Then, the site with same coordinates for size $(N+1)$ (now belonging to sublattice A) is connected to its neighbors along the corresponding $(-\hat{\boldsymbol{\delta}}_j)$

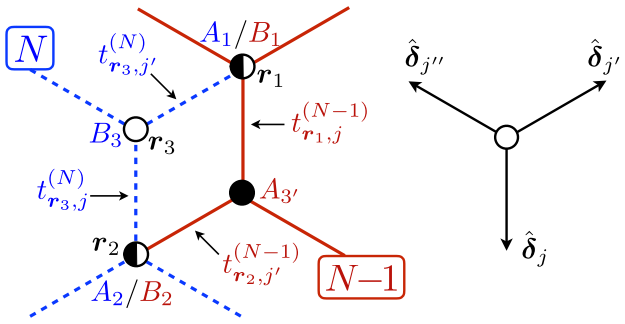

FIG. 3. Illustration of the two different hopping paths (here, exemplarily, $d = 2$): (i) the amplitude from A_1 to A_2 via B_3 along the blue bonds (for size N) is identical to (ii) the amplitude from B_1 to B_2 via $A_{3'}$ along the red bonds (for the size $N-1$). Filled (open) circles denote A (B) sites.

directions via bonds of amplitude $t^{(N+1)}_{\boldsymbol{r}',j}$, where $\boldsymbol{r}' = \boldsymbol{r} - \hat{\boldsymbol{\delta}}_j$. These hoppings obey $t^{(N+1)}_{\boldsymbol{r}',j} = t^{(N)}_{\boldsymbol{r},j} + 1$ because

$$\frac{N - d\boldsymbol{r}' \cdot \hat{\boldsymbol{\delta}}_j}{d+1} - \frac{N - 1 - d\boldsymbol{r} \cdot \hat{\boldsymbol{\delta}}_j}{d+1} = 1. \tag{7}$$

Next, we determine the difference of the diagonal entries of the matrices A_N and B_{N-1}. To that end, we abbreviate the $(d+1)$ hopping amplitudes surrounding an arbitrary A site for size N as $t^{(N)}_1, t^{(N)}_2, \ldots, t^{(N)}_{d+1}$. They satisfy the sum rule $\sum_{j=1}^{d+1} t^{(N)}_j = N + d - 1$ [13]. Furthermore, the site's diagonal entry into A_N is given by $\sum_{j=1}^{d+1} (t^{(N)}_j)^2$. As noted, for the size $(N-1)$, the hopping amplitudes surrounding the corresponding B satisfy $t^{(N-1)}_j = t^{(N)}_j - 1$. Hence, the desired difference of the diagonal entries is

$$\sum_{j=1}^{d+1} [(t^{(N)}_j)^2 - (t^{(N-1)}_j)^2] = \sum_{j=1}^{d+1} [2t^{(N)}_j - 1] = 2N + d - 3. \tag{8}$$

It remains to show that all off-diagonal entries in A_N and B_{N-1} are identical. We consider two arbitrary adjacent B sites for size $(N-1)$ and label them B_1 and B_2. For the size N, the A sites with identical coordinates be A_1 and A_2; for an explicit illustration of $d = 2$, see Fig. 3. The hopping from B_1 to B_2 is via an A site $(A_{3'})$ along the trajectory $\hat{\boldsymbol{\delta}}_j - \hat{\boldsymbol{\delta}}_{j'}$, and the amplitude is $t^{(N-1)}_{\boldsymbol{r}_1,j} t^{(N-1)}_{\boldsymbol{r}_2,j'}$. As the network of $\hat{\boldsymbol{\delta}}_j$ bonds between the sites has been locally inverted when switching from size $(N-1)$ to N, the hopping from A_1 to A_2 is via a B site (B_3) along the trajectory $-\hat{\boldsymbol{\delta}}_{j'} + \hat{\boldsymbol{\delta}}_j$, with the amplitude $t^{(N)}_{\boldsymbol{r}_3,j'} t^{(N)}_{\boldsymbol{r}_3,j}$. From Fig. 3, we see that $\boldsymbol{r}_1 = \boldsymbol{r}_3 + \hat{\boldsymbol{\delta}}_{j'}$ and $\boldsymbol{r}_2 = \boldsymbol{r}_3 + \hat{\boldsymbol{\delta}}_j$. Using $\hat{\boldsymbol{\delta}}_j \cdot \hat{\boldsymbol{\delta}}_{j'} = -(1/d)$ and Eq. (3), we obtain $t^{(N-1)}_{\boldsymbol{r}_1,j} = t^{(N)}_{\boldsymbol{r}_3,j}$ and $t^{(N-1)}_{\boldsymbol{r}_2,j'} = t^{(N)}_{\boldsymbol{r}_3,j'}$. Since the considered hoppings are identical, the pairwise products entering the matrices A_N and B_{N-1} are identical, too. This concludes the proof of Eq. (6).

Step 3: A direct consequence of Eq. (5) and the Lieb-Sutherland theorem is that the spectrum of B_N is given by the one involving A_N plus $z_{d,N}$ zero eigenvalues, where $z_{d,N}$ is the number of excess B sites. Specifically, we have $z_{1,N} = 1$, $z_{2,N} = N$, and $z_{3,N} = N(N+1)/2$; the general expression for $z_{d,N}$, Eq. (4), is derived in the Supplemental Material [13]. Note that the eigenvector structure of the null space (i.e., the zero modes) is nontrivial and generally not known.

Step 4: From Eq. (6), it follows that

$$E^2_n(N) = \sum_{\mu=n+1}^{N} \lambda(\mu) = N(N+d-2) - n(n+d-2), \tag{9}$$

and we obtain the previously proposed spectrum of $\mathcal{H}^2_N$.

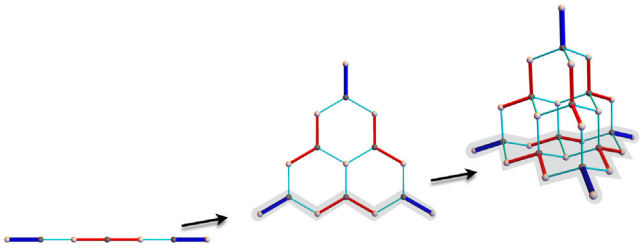

FIG. 4. Dimensional iteration of the d-dimensional simplices. The d-dimensional simplex is constructed from N $(d-1)$-dimensional simplices. For instance, the triangle $(d = 2)$ consists of a chain $(d = 1)$ with $N = 4$, one with $N = 3$, one with $N = 2$, and one with $N = 1$. Correspondingly, the tetrahedron $(d = 3)$ consists of several triangles. This dimensional dependence manifests itself in the expressions for degeneracies, Eq. (4), and the number of lattice sites [13]; see the text.

Step 5: Finally, we show that the degeneracies of the levels at nonzero energy are indeed given by Eq. (4). This follows from the iterative construction: The $z_{d,N}$ zero modes of size N become, upon increasing the size to $(N+1)$, the $2z_{d,N}$ states with energy $E^2_N(N+1) = \lambda(N+1)$ ($z_{d,N}$ states on both of the sublattices A and B), while there are $z_{d,N+1}$ zero modes, etc. As a cross-check, we determine the total number of states for size N: This is $z_{d,N} + \sum_{n=1}^{N-1} 2z_{d,n}$, which equals the number of lattice sites, $M_{d,N}$, and thus the Hilbert space dimension [13]. Hence, there cannot be additional energy levels. This completes the proof.

Dimensional hierarchy.—It is instructive to consider a dimensional iteration, Fig. 4. A chain $(d = 1)$ of size N has one zero mode and consists of $(2N-1)$ sites. A triangle $(d = 2)$ of size N consists of N chains (all with different length, but one excess B site); thus, there are N zero modes and $\sum_{j=1}^{N}(2j-1) = N^2$ sites. Similarly, a tetrahedron $(d = 3)$ of size N consists of N triangles (all with different size), yielding $\sum_{j=1}^{N} j = N(N+1)/2$ zero modes and $\sum_{j=1}^{N} j^2 = N(N+1)(2N+1)/6$ sites. This dimensional iteration allows us to recover the general results for $z_{d,N}$, Eq. (4), and for $M_{d,N}$, as detailed in the Supplemental Material [13]. It also enables a hierarchical construction of the lattices, i.e., of the vectors $\hat{\boldsymbol{\delta}}_j$. In $d = 1$, the two nearest-neighbor displacements are $\hat{\boldsymbol{\delta}}_{1,2} = \pm\hat{\boldsymbol{x}}$. In $(d-1)$ dimensions, the d unit vectors $\hat{\boldsymbol{\delta}}_j$ satisfy $\hat{\boldsymbol{\delta}}_j \cdot \hat{\boldsymbol{\delta}}_{j'} = -1/(d-1)$ for $j \neq j'$. Now define $\hat{\boldsymbol{\delta}}'_j = \sqrt{1 - d^{-2}}\hat{\boldsymbol{\delta}}_j - d^{-1}\hat{\boldsymbol{e}}_d$ and $\hat{\boldsymbol{\delta}}'_{d+1} = \hat{\boldsymbol{e}}_d$, where $\hat{\boldsymbol{e}}_d$ is the unit vector in the dth dimension. Then $\{\hat{\boldsymbol{\delta}}'_j, \ldots, \hat{\boldsymbol{\delta}}'_{d+1}\}$ are the nearest-neighbor unit vectors in d dimensions.

Conclusion.—We have introduced and analyzed a family of tight-binding models for specific finite-size lattices in an arbitrary dimension d where strain-induced inhomogeneous hopping leads to perfectly degenerate PLLs. This is remarkable in two respects. (i) Degenerate Landau levels

usually only follow from (approximate) continuum theories, while lattice models yield only approximately degenerate Landau levels. In contrast, here we have a lattice realization of perfect degeneracies. (ii) While Landau levels in $d = 2$ may be realized using either magnetic field or strain, there is no magnetic-field route in $d = 3$. Hence, our PLL construction provides a unique way of obtaining perfectly flat bands in three dimensions. Upon including electron-electron interactions, flat bands open the exciting possibility of studying fractionalization in three spatial dimensions, similar to what has been done in $d = 2$ for strained graphene [22–24]. This will be the subject of future work. We note that pseudomagnetic fields and the associated pseudo-Landau levels in $d = 1$, 2, 3 could, in principle, be realized in cold-atom settings [25,26], which also enable tunable interactions.

We thank C. Poli, H. Schomerus, W. Lang, and C. Timm for discussions and L. Fritz for previous collaborations on related topics. This research was supported by the DFG through Grants No. SFB 1143, No. SPP 1666, and No. GRK 1621, as well as by the Helmholtz association through Grant No. VI-521. D. P. A. is grateful for the hospitality of the ITP and SFB 1143 at TU Dresden.

[1] K. K. Gomes, W. Mar, W. Ko, F. Guinea, and H. C. Manoharan, Nature (London) **483**, 306 (2012).
[2] N. Reyren *et al.*, Science **317**, 1196 (2007).
[3] J. Chakhalian, J. W. Freeland, A. J. Millis, C. Panagopoulos, and J. M. Rondinelli, Rev. Mod. Phys. **86**, 1189 (2014).
[4] C. L. Kane, R. Mukhopadhyay, and T. C. Lubensky, Phys. Rev. Lett. **88**, 036401 (2002).
[5] M. M. Fogler, F. Guinea, and M. I. Katsnelson, Phys. Rev. Lett. **101**, 226804 (2008).
[6] F. Guinea, M. I. Katsnelson, and A. K. Geim, Nat. Phys. **6**, 30 (2010).
[7] M. Vozmediano, M. Katsnelson, and F. Guinea, Phys. Rep. **496**, 109 (2010).
[8] N. Levy, S. A. Burke, K. L. Meaker, M. Panlasigui, A. Zettl, F. Guinea, A. H. Castro-Neto, and M. F. Crommie, Science **329**, 544 (2010).
[9] D. I. Pikulin, A. Chen, and M. Franz, Phys. Rev. X **6**, 041021 (2016).
[10] A. Cortijo, D. Kharzeev, K. Landsteiner, and M. A. H. Vozmediano, arXiv:1607.03491.
[11] A. G. Grushin, J. W. F. Venderbos, A. Vishwanath, and R. Ilan, arXiv:1607.04268 [Phys. Rev. X (to be published)].
[12] C. Poli, J. Arkinstall, and H. Schomerus, Phys. Rev. B **90**, 155418 (2014).
[13] See Supplemental Material at http://link.aps.org/supplemental/10.1103/PhysRevLett.117.266801 for details of the proof and for numerical data for finite electron-lattice coupling.
[14] M. Neek-Amal, L. Covaci, Kh. Shakouri, and F. M. Peeters, Phys. Rev. B **88**, 115428 (2013).
[15] D. J. Chadi and M. L. Cohen, Phys. Status Solidi (b) **68**, 405 (1975).
[16] S. Rachel, D. P. Arovas *et al.* (to be published).
[17] If the number of zero modes exceeds $|n_B - n_A|$, the additional number of zero modes must be even.
[18] B. Sutherland, Phys. Rev. B **34**, 5208 (1986).
[19] E. H. Lieb, Phys. Rev. Lett. **62**, 1201 (1989).
[20] M. Inui, S. A. Trugman, and E. Abrahams, Phys. Rev. B **49**, 3190 (1994).
[21] The normalized real eigenvectors ϕ_A and ϕ_B are defined up to an overall sign. A change $\phi_A \to -\phi_A$ or $\phi_B \to -\phi_B$ leads to $E_n \to -E_n$ in Eq. (5).
[22] P. Ghaemi, J. Cayssol, D. N. Sheng, and A. Vishwanath, Phys. Rev. Lett. **108**, 266801 (2012).
[23] D. A. Abanin and D. A. Pesin, Phys. Rev. Lett. **109**, 066802 (2012).
[24] J. W. F. Venderbos and L. Fu, Phys. Rev. B **93**, 195126 (2016).
[25] W. S. Bakr, J. Gillen, A. Peng, S. Fölling, and M. Greiner, Nature (London) **462**, 74 (2009).
[26] C. Muldoon, L. Brandt, J. Dong, D. Stuart, E. Brainis, M. Himsworth, and A. Kuhn, New J. Phys. **14**, 073051 (2012).